35th Annual International Conference of the IEEE EMBS
Osaka, Japan, 3 - 7 July, 2013

Bubble-Driven Light-Absorbing Hydrogel Microrobot for the Assembly of Bio-Objects

Wenqi Hu, *Student Member*, *IEEE*, Qihui Fan, *Student Member*, *IEEE*,
Wade Tonaki, *Student Member*, *IEEE,* and Aaron T. Ohta, *Member, IEEE*

***Abstract*— Microrobots made of light-absorbing hydrogel material were actuated by optically induced thermocapillary flow and move at up to 700 µm/s. The micro-assembly capabilities of the microrobots were demonstrated by assembling polystyrene beads and yeast cells into various patterns on standard glass microscope slides. Two microrobots operating independently in parallel were also used to assemble micro-hydrogel structures.**

I. Introduction

Microrobotics is an emerging field that uses untethered actuators as tools for the micro-manipulation [1-3] and micro-assembly of bio-objects such as living cells [4], [5], and micro-hydrogel structures with embedded cells [5]. Microrobot actuation mechanisms that have been demonstrated include magnetic fields [4], [6], electrical fields [7], and harnessing motile bacteria [8].

As a highly condensed and easily re-directed energy source, light is widely used to trap bio-samples directly, using technologies such as optical tweezers [9]. However, overexposure of the samples to the incident light may cause damage [10]. To address this, microtools, which are made of patterned SU-8 or self-assembled beads, are actuated by multi-beam optical tweezers to manipulate bio-samples [11], [12]. Another toolset that can accomplish this task are hydrogel microrobots, which are driven by optically induced bubbles [5]. These microrobots consist of disks approximately 100 µm in diameter made of poly(ethylene glycol) diacrylate, or PEGDA, a biocompatible hydrogel. The microrobots reside in an uncovered fluidic reservoir on an absorbing substrate. Bubbles less than 10 µm in diameter were created by a laser to actuate the hydrogel microrobots by pushing on a dimple in the center of the disk.

The hydrogel microrobots feature straightforward optical control, and parallel manipulation was demonstrated by using multiple light spots, one per microrobot. Additionally, the hydrogel microrobots are biocompatible, and can safely manipulate living cells. Finally, they are also able to operate in an open fluidic reservoir, facilitating access to the micro-assembled objects. Nevertheless, the requirement of a light-absorbing substrate for hydrogel microrobot actuation poses some limitations on its applications in, for example, typical cell culture flasks made of polystyrene. To address this, a less substrate-dependent hydrogel microrobot is necessary.

Thus, here we report the actuation of a bubble-driven, light-absorbing microrobot (BLM) in a phosphate buffered saline (PBS) solution. Instead of using a light-absorbing substrate, the microrobot itself absorbs light, and the same optically induced thermocapillary flow used for the hydrogel microrobots can be created around and actuate the BLM. This new microrobot expands the applicability of optically actuated microrobots in biomedical research.

II. Setup and Actuation Mechanism

The setup of the BLM system is shown in Fig. 1. A standard microscope glass slide (75mm × 25mm × 1mm) is placed on the specimen stage under an Olympus BXFM upright microscope. A 980-nm infrared laser (Laserlands, 980MD-0.8W-BL) is mounted on an XYZ stage positioned below the microscope stage. The on-off states of the laser can be switched by a TTL signal from a function generator. The

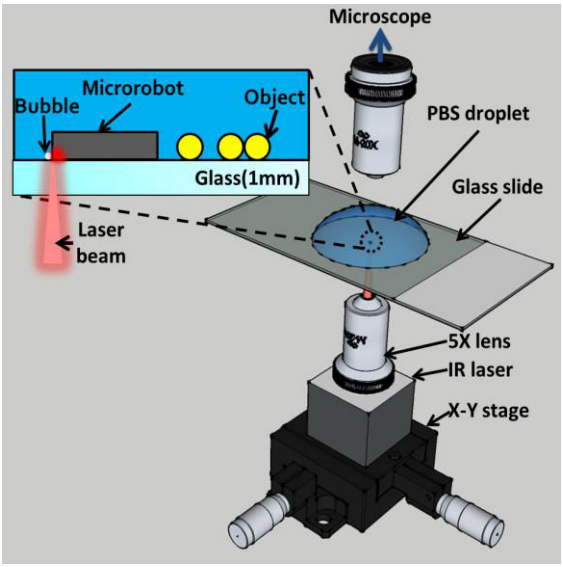

Fig. 1. The bubble-driven light-absorbing microrobot system. The inset shows the side view of the microrobot. The 980-nm infrared diode laser was focused on the edges of the absorbing microrobot to create bubbles and thermocapillary flow along the bubble surface, actuating the microrobots.

This work was supported by Grant Number 1R01EB016458-01 from the National Institute of Biomedical Imaging and Bioengineering of the National Institutes of Health (NIH). These contents are solely the responsibility of the authors and do not necessarily represent the official views of the NIH.

W. Hu, W. Tonaki, and A. T. Ohta are with the Department of Electrical Engineering, University of Hawai‘i at Manoā, Honolulu, HI 96822, USA (808-341-0260; fax: 808-956-3427; e-mails: wenqihu@hawaii.edu, wtonaki@hawaii.edu, aohta@hawaii.edu.

Q. Fan is with the Department of Mechanical Engineering, University of Hawai‘i at Manoā, Honolulu, HI 96822 USA (e-mail: fanqihui@hawaii.edu).

laser is focused by a 5X objective lens (Newport, N.A. = 0.1) into a circular spot with a full-width at half-maximum (FWHM) diameter of 17.6 μm. Note that the magnification and numerical aperture of the objective lens used here is significantly smaller than that in optical tweezers setup (usually above 40 X and 1.4 N.A.) [12]. When the laser was on, the measured intensity at the focal point is 72 kW/cm^2.

The BLM used in the experiments presented here was made of a T-shaped ink-dyed PEGDA hydrogel, approximately 20 μm in thickness. It was created in a photopolymerization procedure adapted from ref. [13]. The prepolymer consists of a mixture of two parts PEGDA (Sigma Aldrich, typical M_n: 575) with 1% Irgacure 819 photoinitiator (Ciba Specialty Chemicals Inc.), and one part pigmented ink (Higgins Black India ink). India ink is biocompatible [14] and contains carbon black nanoparticles that absorb light. The geometry of the BLM can be divided into two rectangular sections, "A" and "B" (Fig. 2). Two types of BLM were tested. The dimensions of each are: Type 1, $W_A = 75$ μm, $L_A = 200$ μm, $W_B = 75$ μm, $L_B = 150$ μm; Type 2, $W_A = 30$ μm, $L_A = 115$ μm, $W_B = 45$ μm, $L_B = 80$ μm. The larger Type 1 BLM is designed for the manipulation of objects larger than 10 μm while the Type 2 BLM is intended for the manipulation of smaller objects such as yeast cells.

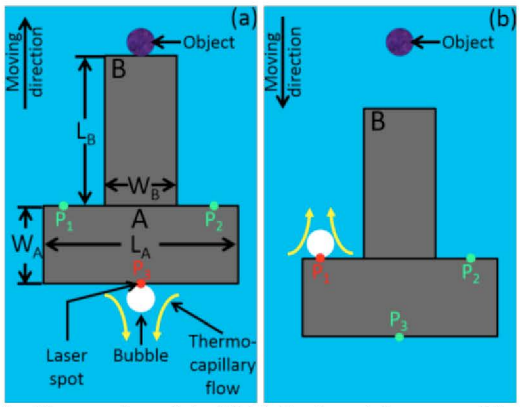

Fig. 2. The top view of the BLM. P_1, P_2 and P_3 are possible laser stimulation points for driving the BLM forward and backward. The point activated by the laser is marked in red. The thermocapillary flow is indicated by the yellow arrows. (a) Laser stimulation at P_3 will move the microrobot forward (towards the top of the drawing). (b) Laser stimulation that alternates between at P_1 and P_2 will move the microrobot backward (towards the bottom of the drawing).

To move the BLM forward (towards the top of Fig. 2), the laser is focused on the bottom edge of bar "A" (P_3 in Fig. 2a). The laser-induced heating creates cavitation bubbles at the edge of the microrobot structure. The surface of the generated bubble is hotter at the side closest to the edge of bar "A", and is cooler on the side farthest from bar "A". This temperature gradient around the gas/liquid interface drives a thermocapillary flow [15] and pushes the bubble towards the hotter side, which is against the edge of the BLM. Maintaining the focal point at the BLM edge maintains the thermocapillary flow, driving the BLM forward. It should be noted that this mechanism is fundamentally different from the bubble thrust reported in ref. [16]. The orientation of the BLM can be changed by stimulating different areas along the perimeter of the BLM, enabling steering and other functions. The laser can also stimulate the top edge of the bar "A" to move the BLM backwards and away from the object (P_1 in Fig. 2b). However, continuous stimulation at P_1 can cause the BLM rotate counterclockwise. This rotation is prevented by alternating the stimulation between P_1 and another point on bar "A" (P_2 in Fig. 2b).

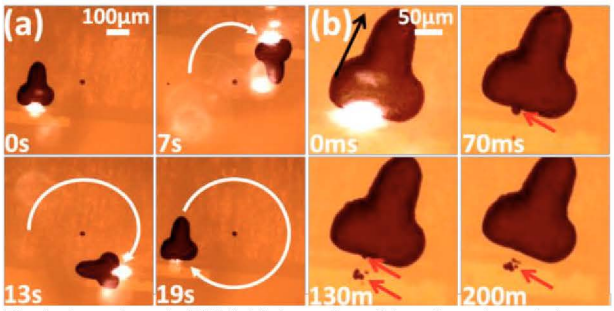

Fig. 3. Actuation of a BLM. (a) Actuation of the microrobot relative to a 20-μm-diameter polystyrene bead in the center of the field of view. The movement path is marked by the white arrows. (b) A closer view of the microrobot actuation, taken from video frames immediately after the first frame in (a), showing the cavitation bubble created by the laser that enables the thermocapillary flow. The direction of the microrobot movement is marked by a black arrow. The cavitation bubbles are marked by red arrows.

Two-dimensional BLM motion was demonstrated by moving a Type 1 BLM around a 20-μm-diameter polystyrene bead (Fig. 3a). Light diffraction in the photopolymerization system rounded the edges of this particular microrobot. The BLM was in a 500-μl droplet of PBS on a glass microscope slide. A 200-Hz pulse train was sent to the laser control circuit to switch the laser on and off. The frame rate of the microscope camera was set to 201 Hz. This made the laser appear on the camera at a frequency of 1 Hz, enabling observation of the laser spot and the optically induced cavitation bubble. With a 250 μs laser pulse width, the microrobot finished moving along the circular path in 19 seconds, at an average velocity of 150 μm/s.

The optically induced cavitation bubbles can be observed during the microrobot actuation (Fig. 3b). Note that, except for the first frame, the laser is not visible, due to the discrepancy between the microscope camera frame rate and the frequency of the control signal. Since PEGDA is hydrophilic, the bubbles detached from the BLM surface between laser pulses, when there was no thermocapillary flow pushing the bubbles against the microrobot. The bubbles were then circulated away by the thermocapillary flow affiliated with the next newly generated bubble (seen in the 70 ms and 130 ms frames in Fig. 3b), and dissolved into the medium due to Laplace pressure.

By tuning the pulse width, the duration of the thermocapillary flow in each period of the control signal can be adjusted. As the pulse width is increased, so is the microrobot actuation velocity (Fig. 4). Thus, if a fine

adjustment of the microrobot orientation is necessary, the pulse width can be lowered, allowing more precision.

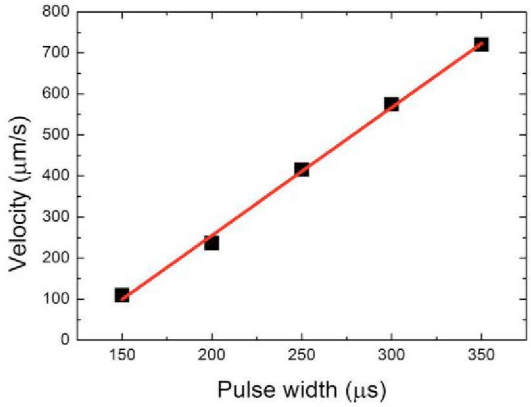

Fig. 4. Measured velocity of a Type 1 light-absorbing microrobot as a function of the laser pulse width. A red linear trend line was added.

III. Micro-manipulation Results

A. Assembly of Polystyrene Beads

To demonstrate the micro-assembly capability of the BLM, ten 20-μm-diameter polystyrene beads were assembled into a densely packed "H" pattern, for "Hawaii" (Fig. 5). The Type 1 BLM was used for this micro-assembly procedure. The pulse width was 350 μs and the entire assembly process took about half an hour.

It took less than seven minutes to assemble the first five beads (Fig. 5b). However, it took another ten minutes to place the next two beads in the desired location (Fig. 5c). This is due to the rounded tip of this microrobot (bar "B"). A significant amount of time was consumed as the orientation of the BLM was constantly adjusted to maintain the beads at the center of the tip while moving the microrobot in the desired direction. The manipulation velocity when pushing a single bead in straight line was up to 44 μm/s. This velocity is slower than the movement of the BLM by itself, partly due to this reorientation issue. The actuation of the BLM was also slowed by the accidental generation of bubbles underneath the BLM. The insets in Fig. 5c highlight two bubbles that were generated underneath the BLM. A bubble created underneath the BLM may lift the microrobot off the substrate, making it difficult to maintain the laser focus at the edge of the microrobot. If a bubble is created below the microrobot, actuation may be temporarily interrupted. The BLM can recover, as long as enough time has elapsed for the bubbles to dissolve into the medium.

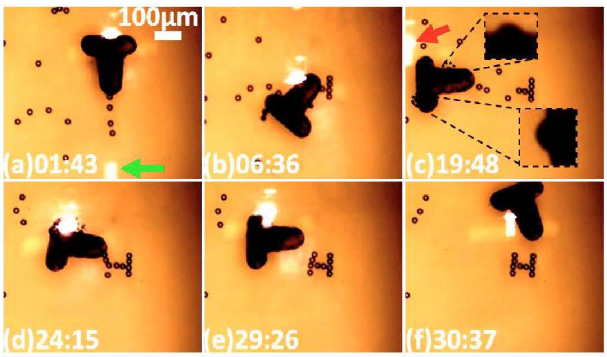

Fig. 5. Micro-assembly of 20-μm-diameter polystyrene beads into "H" shape. The time stamp format is minutes : seconds. (a, b) Assembly of the right half of the "H" pattern. The rectangular-shaped light bar marked by the green arrow is an artifact due to the difference between the laser pulse train frequency and the camera capture frame rate. (c-d) Assembly of the left half of the "H" pattern. The laser spot position is marked by a red arrow in (c). The inset shows the bubble trapped at the bottom of the microrobot. (e-f) Fine adjustment of the assembled beads.

The assembly of the "H" was nearly complete after 25 minutes (Fig. 5d). Another five minutes was used to pack the beads in a denser arrangement (Fig. 5e, f). During this process, the pulse width was decreased to 200 μs to achieve more precise control of the BLM.

B. Manipulation of Single Yeast Cells

A tool for single-cell manipulation can be useful in biological research [17]. The BLM has potential as a tool for single cell manipulation. To demonstrate this ability, baker's yeast was used as a model cell. Three yeast cells with an average diameter of 8 μm were aligned by a Type 2 BLM into a straight line (Fig. 6).

The ambient temperature for this experiment was 20 °C. The temperature at the tip of bar "B", where the cells contact the BLM, is less than 32 °C, verified by the method described in [5]. The manipulation took approximately seven and a half minutes, and the peak manipulation velocity for pushing the yeast in straight line was 18 μm/s. This was due to the same issues mentioned in regards to manipulating the polystyrene beads. In addition, the positions of the cells were also disturbed by the fluid flows around the BLM during movement [6]. To avoid this, the BLM had to move slowly when it was in close proximity to the assembled cells. This was especially important during the final positioning of cells. After putting a cell into its final location, the BLM actuation was paused for 10 to 20 seconds to allow the cell settle down on the substrate.

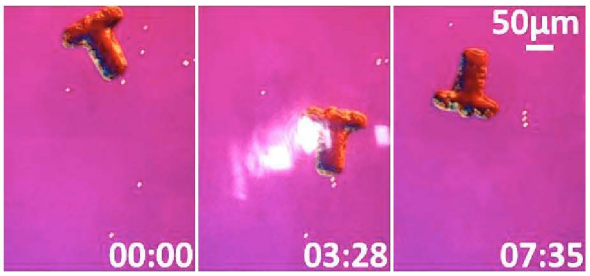

Fig. 6. Manipulation of single yeast cells. Yeast cells are seen as white dots in the frames. The time stamp format is minutes : seconds.

C. Parallel Manipulation of Micro-hydrogels

Micro-scale hydrogels, or microgels, are useful as cellular scaffolds for tissue engineering. Organizing cell-laden microgels into certain geometries, followed by cell culturing, mimics how cells in the human body arrange themselves and

develop into a tissue [18].

Agarose is a widely used bio-matrix for supporting cell growth in 3D [19], and can be used to create cell-laden microgels. Agarose microgels were assembled using the absorbing microrobots as a proof-of-concept of the assembly of cell-laden microgel constructs (Fig. 8).

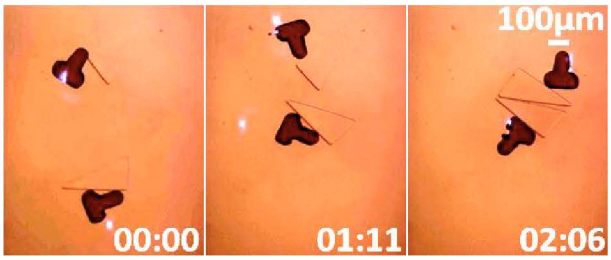

Fig. 8. Parallel, cooperative assembly of two triangular agarose microgels. The time stamp format is minutes : seconds.

Triangular agarose (3%, Sigma Aldrich, Type IX-A) microgels were fabricated according to the method in ref. [4]. Two Type 1 BLMs were used to manipulate the agarose microgels in parallel and independently. To enable the operation, an additional laser was added to the setup so that the two lasers projected obliquely onto the glass microscope slide. A separate person operated each laser, addressing a single BLM. The users coordinated BLM movements to arrange two triangular agarose hydrogels into a rectangular shape (Fig. 8). The maximum manipulation velocity in straight line was 6 µm/s, as the microgels are larger than polystyrene beads and yeast cells. To achieve a higher manipulation speed, a longer laser pulse width could be used, but this carries the risk of overheating and damaging the BLM.

IV. Conclusion and Future Work

In this report, light-absorbing hydrogel microrobots driven by optically induced thermocapillary flow were demonstrated. The BLMs were bio-compatible and easily fabricated in single-step photopolymerization procedure. The BLMs were used to manipulate polystyrene beads and single yeast cells on a standard glass microscope slide. Cooperative manipulation of triangular microgels by two BLMs was also achieved.

The current fabrication procedures and design of BLM can be optimized further, helping to increase its mechanical strength and assembly speed. Lower-molecular-weight PEGDA forms a more robust hydrogel [20], which permits using longer laser pulse widths for stronger actuation forces. Another modification that can be made is the addition of a structure to better retain micro-objects on the tip of the BLM, reducing the time spent on re-orienting the BLM during micro-assembly. The current open-loop control of the BLMs also contributes to the assembly time.

References

[1] W. Hu, K. S. Ishii, and A. T. Ohta, "Micro-assembly using optically controlled bubble microrobots," *Applied Physics Letters*, vol. 99, p. 094103, 2011.

[2] K. S. Ishii, W. Hu, and A. T. Ohta, "Cooperative micromanipulation using optically controlled bubble microrobots," *in IEEE International Conference on Robotics and Automation*, 2012, pp. 3443-3448.

[3] W. Hu, K. S. Ishii, and A. T. Ohta, "Micro-assembly using optically controlled bubble microrobots in saline solution," in *IEEE International Conference on Robotics and Automation*, 2012, pp. 733–738.

[4] M. S. Sakar, E. B. Steager, A. Cowley, V. Kumar, and G. J. Pappas, "Wireless manipulation of single cells using magnetic microtransporters," in *IEEE International Conference on Robotics and Automation*, 2011, pp. 2668–2673.

[5] W. Hu, K. S. Ishii, Q. Fan, and A. T. Ohta, "Hydrogel microrobots actuated by optically generated vapour bubbles," *Lab on a Chip*, vol. 12, no. 19, pp. 3821–3826, 2012.

[6] S. Floyd, C. Pawashe, and M. Sitti, "Two-dimensional contact and noncontact micromanipulation in liquid using an untethered mobile magnetic microrobot," *IEEE Transactions on Robotics*, vol. 25, no. 6, pp. 1332–1342, Dec. 2009.

[7] B. R. Donald, C. G. Levey, and I. Paprotny, "Planar microassembly by parallel actuation of MEMS microrobots," *Journal of Microelectromechanical Systems*, vol. 17, no. 4, pp. 789–808, 2008.

[8] E. B. Steager, M. S. Sakar, D. H. Kim, V. Kumar, G. J. Pappas, and M. J. Kim, "Electrokinetic and optical control of bacterial microrobots," *Journal of Micromechanics and Microengineering*, vol. 21, no. 3. p. 035001, 2011.

[9] J. R. Moffitt, Y. R. Chemla, S. B. Smith, and C. Bustamante, "Recent advances in optical tweezers," *Annual Review of Biochemistry*, vol. 77, pp. 205–28, Jan. 2008.

[10] S. K. Mohanty, A. Rapp, S. Monajembashi, P. K. Guptaa, and K. O. Greulichb, "Comet assay measurements of DNA damage in cells by laser microbeams and trapping beams with wavelengths spanning a range of 308 nm to 1064 nm," *Radiation Research*, vol. 157, no. 4, pp. 378–385, 2009.

[11] F. Arai, T. Sakami, H. Maruyama, A. Ichikawa, and T. Fukuda, "Minimally invasive micromanipulation of microbe by laser trapped micro tools," in *IEEE International Conference on Robotics and Automation*, 2002, pp. 1937-1942.

[12] H. Maruyama, R. Iitsuka, K. Onda, and F. Arai, "Massive parallel assembly of microbeads for fabrication of microtools having spherical structure and powerful laser manipulation," in *IEEE International Conference on Robotics and Automation*, 2010, pp. 482–487.

[13] S. E. Chung, W. Park, H. Park, K. Yu, N. Park, and S. Kwon, "Optofluidic maskless lithography system for real-time synthesis of photopolymerized microstructures in microfluidic channels," *Applied Physics Letters*, vol. 91, no. 4, p. 041106, 2007.

[14] B. A Shatz, L. B. Weinstock, P. E. Swanson, and E. P. Thyssen, "Long-term safety of India ink tattoos in the colon," *Gastrointestinal Endoscopy*, vol. 45, no. 2, pp. 153–156, 1997.

[15] V. G. Levich, *Physicochemical Hydrodynamics*. Englewood Cliffs, NJ: Prentice-Hall, Inc., 1962.

[16] J. Wang and W. Gao, "Nano/Microscale motors: biomedical opportunities and challenges.," *ACS Nano*, vol. 6, no. 7, pp. 5745–51, 2012.

[17] S. Hong, Q. Pan, and L. P. Lee, "Single-cell level co-culture platform for intercellular communication," *Integrative Biology : quantitative biosciences from nano to macro*, vol. 4, no. 4, pp. 374–380, 2012.

[18] Y. Du, E. Lo, S. Ali, and A. Khademhosseini, "Directed assembly of cell-laden microgels for fabrication of 3D tissue constructs," *Proceedings of the National Academy of Sciences of the United States of America*, vol. 105, no. 28, pp. 9522–9527, 2008.

[19] D. R. Albrecht, G. H. Underhill, T. B. Wassermann, R. L. Sah, and S. N. Bhatia, "Probing the role of multicellular organization in three-dimensional microenvironments," *Nature Methods*, vol. 3, no. 5, pp. 369-375, 2006.

[20] J. P. Mazzoccoli, D. L. Feke, H. Baskaran, and P. N. Pintauro, "Mechanical and cell viability properties of crosslinked low- and high-molecular weight poly(ethylene glycol) diacrylate blends," *Journal of Biomedical Materials Research Part A*, vol. 93, no. 2, pp. 558–66, 2010.